AIAA SciTech Forum
7-11 January 2019, San Diego, California
AIAA Scitech 2019 Forum

10.2514/6.2019-0168

Towards Aerodynamic Shape Optimization of Unsteady Turbulent Flows

Anthony Ashley*, Jared Crean†, and Jason Hicken‡
Rensselaer Polytechnic Institute

Optimization is an important phase of modern engineering design, and gradient-based optimization methods are especially effective for design problems involving a large number of design variables, such as aerodynamic shape optimization. However, if the system of interest exhibits chaotic dynamics and the quantity of interest is a long-time average, for example, drag in a turbulent flow, conventional sensitivity analysis methods will fail to provide useful gradients and gradient-based optimization becomes infeasible. Progress has been made in the sensitivity analysis of chaotic systems, but most proposed methods are computationally expensive. We propose a new method of stabilizing the tangent-sensitivity equations by introducing a minimal perturbation to the linearized equations. The goal is to eliminate linear instabilities in the sensitivity equations, while ensuring useful gradients are obtained. We implement the tangent sensitivity method on a model chaotic problem, demonstrate the effectiveness of our stabilizations, and validate the gradient information obtained from the stabilized tangent sensitivity. Finally, we describe how the method of stabilization can easily be adapted to the sensitivity analysis of large-scale computational fluid dynamics problems.

I. Introduction

Turbulent flows are ubiquitious in aerospace applications; for example, they are found in boundary layers, shear layers, and combustion chambers. Furthermore, there is strong impetus to design for and control turbulent flows, because the enhanced mixing and momentum transport can have a significant impact, both good and bad, on performance. To this end, we are interested in using aerodynamic shape optimization (ASO) to improve the performance of systems subject to turbulent flows. ASO problems, in particular, typically involve a large number of design variables, so gradient-based optimization methods are desirable because they have excellent algorithmic scaling.

Historically, the challenge of gradient-based ASO has been the implementation of sensitivity analysis methods to obtain the derivatives of the objective and constraints. The conventional finite-difference and complex-step [1] methods, while intuitive and easy to implement, scale linearly with the number of design variables. Adjoint-based methods [2, 3], on the other hand, are effective at calculating derivatives with a computational cost virtually independent of the number of design variables. These methods are well established for steady flows and are being increasingly used for unsteady flows [4–7]. However, there is a class of unsteady problems for which these mature techniques fail to produce useful sensitivities: unsteady, turbulent flows.

Turbulent problems are difficult for conventional sensitivity analysis methods, because turbulent flows are chaotic. Chaotic problems are sensitive to small changes in initial conditions, or other parameters, that govern the nature of the solution. To demonstrate this, consider the Lorenz system [8], which is a simplified model of atmospheric convection. It is a system of ordinary differential equations defined by

$$\frac{d}{dt}\begin{pmatrix} x \\ y \\ z \end{pmatrix} = \begin{pmatrix} \sigma(y-x) \\ x(\rho - z) - y \\ xy - \beta z \end{pmatrix}, \qquad \boldsymbol{x}(0) = \boldsymbol{x}_0. \tag{1}$$

The Lorenz system has three spatial variables, x, y, and z, and three parameters, ρ, β, and σ. This simple-looking system exhibits chaotic behavior for a particular range of parameter values. Figure 1 demonstrates the chaotic nature of the Lorenz system by showing its extreme sensitivity to slight changes in a parameter, in this case ρ. Also shown is the result of a finite-difference gradient computation of the state sensitivity: using a finite-difference step size that would be suitable for a smooth problem results in a large, unusable sensitivity.

*PhD Candidate, Department of Mechanical, Aerospace, and Nuclear Engineering; Student Member AIAA
†PhD Candidate, Department of Mechanical, Aerospace, and Nuclear Engineering; Student Member AIAA
‡Associate Professor, Department of Mechanical, Aerospace, and Nuclear Engineering; Member AIAA

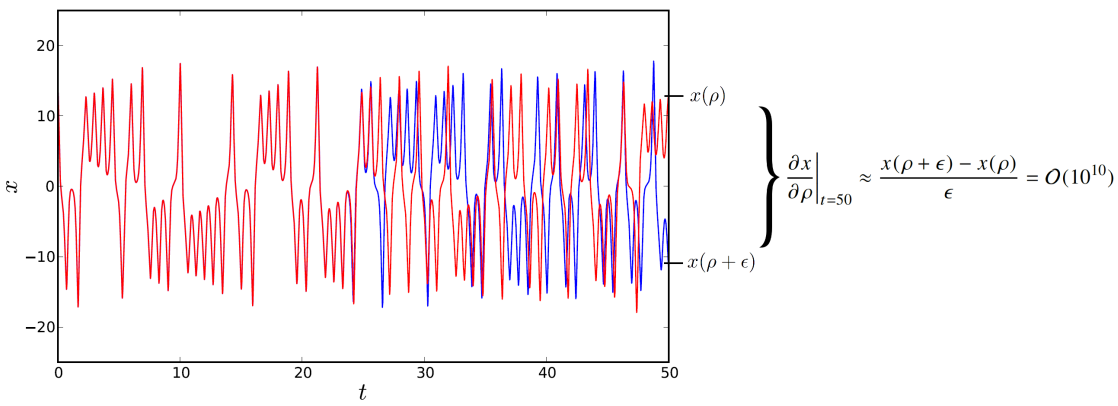

Figure 1 Two solution trajectories of the Lorenz system. The first, in red, is a trajectory based on $\rho = 28.0$, and the second, in blue, is a trajectory based on $\rho = 28.0 + 10^{-10}$. The initial conditions are identical. The rapid divergence of the trajectories, even with such a small parameter perturbation, is apparent. This results in unusable gradient information, as demonstrated to the right.

Several strategies have been investigated to obtain useful sensitivities for chaotic problems. Some of these strategies seek to build off the success of the conventional adjoint method for nonchaotic problems. One such method is the ensemble adjoint method [9, 10], but it has been shown to converge at an unacceptably slow rate [11, 12]. In contrast, the least squares shadowing (LSS) method [13, 14] succeeds in obtaining relatively accurate gradient data for problems exhibiting chaotic dynamics.

The LSS method involves the solution of a space-time saddle-point problem whose size scales with the number of state variables times the number of time steps; in light of this, the LSS method is impractical for most computational fluid dynamics (CFD) applications, and several strategies for reducing its cost have been investigated. The feasibility of approximating the LSS adjoint with Fourier modes was studied in [15], but this approximation still requires an expensive linear solve, as it alters the problem from a large sparse linear system to a smaller dense linear system. The non-intrusive least squares shadowing (NILSS) method [16–18] seeks to address the computational cost of the LSS method, while still computing useful gradient information. While it shows promise, NILSS requires a potentially large (> 100) number of linearized partial differential equation (PDE) solves, one for each positive Lyapunov exponent.

In this work, we introduce a new technique for obtaining gradient information for systems governed by chaotic flows. Instead of taking a shadowing approach to approximating the chaotic trajectory, we seek to stabilize the tangent- or adjoint-sensitivity equation used to compute the gradient. This approach is similar to that of Talniker *et al.* [19], but the method of stabilization differs. The general strategy is to introduce a localized perturbation to the linear tangent or adjoint PDE that seeks to eliminate the instability that leads to unusable gradients. We consider two perturbations, one that removes positive eigenvalues and one that is the smallest possible perturbation that ensures stability; both perturbations can be applied at the element level in a finite-element CFD solver, making them practical for large scale problems.

The remainder of the paper is organized as follows. Section II briefly reviews conventional techniques that are used to obtain gradients and explains why they fail for chaotic problems. We describe the proposed stabilized tangent-sensitivity methods in Section III, and illustrate their performance on a model problem. Section IV discusses how these methods generalize to large-scale CFD problems, and describes some implementation details necessary to achieve this goal. Finally, we summarize the results and draw conclusions in Section V.

II. A review of sensitivity analysis methods

A. Conventional sensitivity analysis methods

In this section, we briefly review the (conventional) tangent and adjoint sensitivity analysis methods; readers familiar with this subject can safely proceed to the next section.

Using bold font to denote a vector quantity, we assume that the state, $\mathbf{u}$, is governed by the time-invariant system

$$\frac{d\mathbf{u}}{dt} - \mathbf{f}(\mathbf{u}, s) = \mathbf{R}(\mathbf{u}, s) = \mathbf{0}, \qquad \mathbf{u}(t = 0) = \mathbf{u_0}. \tag{2}$$

Examples of $\mathbf{f}$ include Navier-Stokes spatial discretizations, and the right hand side of the ordinary differential equation in (1). The parameter s denotes a design variable (such as a shape parameter) and $\mathbf{u_0}$ is a prescribed initial condition.

Given an objective function J, we are interested in evaluating the total derivative dJ/ds. Using the chain rule, we can express this derivative as

$$\frac{dJ}{ds} = \frac{\partial J}{\partial s} + \frac{\partial J}{\partial \mathbf{u}} \frac{d\mathbf{u}}{ds}. \tag{3}$$

To find the state sensitivity $d\mathbf{u}/ds$, we take the total derivative of the residual $\mathbf{R}$ with respect to the parameter s, which gives us

$$\frac{d\mathbf{R}}{ds} = \frac{\partial \mathbf{R}}{\partial s} + \frac{\partial \mathbf{R}}{\partial \mathbf{u}} \frac{d\mathbf{u}}{ds} = \mathbf{0}. \tag{4}$$

Since the total derivative of $\mathbf{R}$ is equal to zero, and assuming the Jacobian $\partial\mathbf{R}/\partial\mathbf{u}$ is invertible, we obtain a linear equation for $d\mathbf{u}/ds$. After solving for $d\mathbf{u}/ds$, the tangent (or direct) sensitivity method then substitutes the value of $d\mathbf{u}/ds$ into (3) to obtain dJ/ds.

Alternatively, we can substitute the expression for $d\mathbf{u}/ds$ from (4) into (3) and obtain

$$\frac{dJ}{ds} = \frac{\partial J}{\partial s} - \frac{\partial J}{\partial \mathbf{u}} \left(\frac{\partial \mathbf{R}}{\partial \mathbf{u}} \right)^{-1} \frac{\partial \mathbf{R}}{\partial s}. \tag{5}$$

The product $(\partial J/\partial \mathbf{u})(\partial \mathbf{R}/\partial \mathbf{u})^{-1}$, which appears in (5), is independent of the dimension of s, and can be computed once and used to obtain gradients with respect to every design variable. This product is called the adjoint, ψ, and it satisfies

$$\frac{\partial \mathbf{R}}{\partial \mathbf{u}}^T \psi = -\frac{\partial J}{\partial \mathbf{u}}^T. \tag{6}$$

Since the calculation of the adjoint variables does not depend on the number of design variables, the adjoint method is very attractive for aerodynamic shape optimization, where the number of design variables is often large. However, compared to the adjoint method, the tangent sensitivity method is easier to implement, and therefore is more suited to the preliminary investigation of our proposed method in this paper.

B. Breakdown of conventional sensitivity methods

The above sensitivity analysis methods work well for smooth problems. However, in the presence of chaotic dynamics, they produce unusable gradients. To demonstrate this, we again consider the Lorenz problem, this time with the objective function

$$J_T(\rho) = \int_0^T \frac{1}{2T} \left(z(t, \rho) - z_{\text{targ}} \right)^2 dt, \tag{7}$$

where we have selected ρ as a design variable and $z_{\text{targ}} = 35$.

Figure 2 shows the result of applying the conventional tangent sensitivity method to the Lorenz system and the objective function (7). The objective function is plotted in grey over a range of ρ values, and overlaid in blue is a linearization of the gradient resulting from the tangent sensitivity method: $\partial J/\partial \rho$. The gradient value given by the tangent sensitivity method at the selected value of ρ is on the order of 10^{18}; clearly, this would be unusable in any gradient-based optimization algorithm and does not reflect the general trent of the objective as a function of ρ.

To understand why the gradient is so large in magnitude, we have plotted the absolute value of one of the components of the tangent sensitivity, $|v_2| = |dy/d\rho|$, versus time in Figure 3. If these values of $\mathbf{v}$ are inserted in (5), we obtain the (unusable) gradient information seen in Figure 2. It is this exponential growth in the sensitivity that we wish to mitigate with our proposed method.

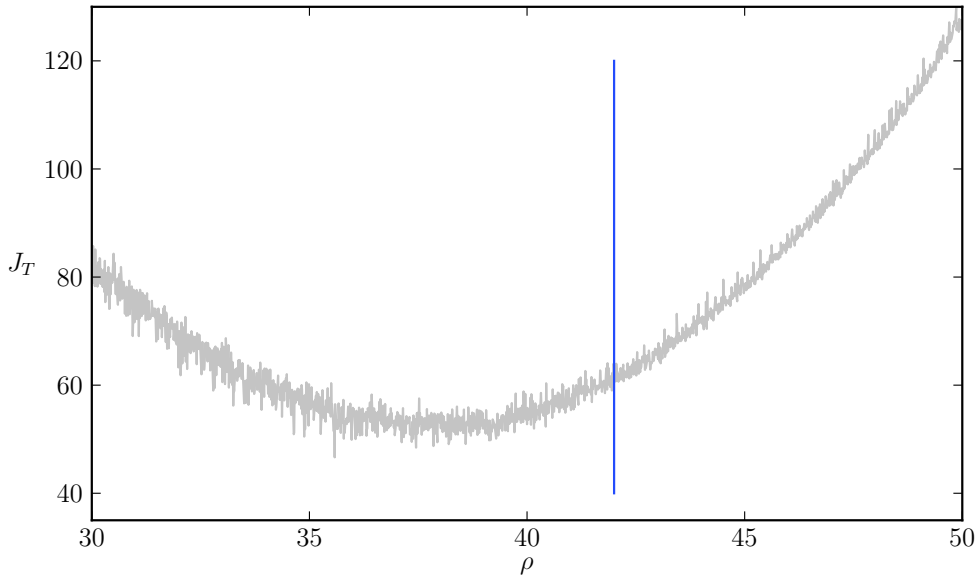

Figure 2 Unusable gradient information obtained from the conventional tangent sensitivity method applied to the Lorenz system. Objective function values are plotted in grey, with the gradient resulting from the tangent sensitivity method overlaid in blue.

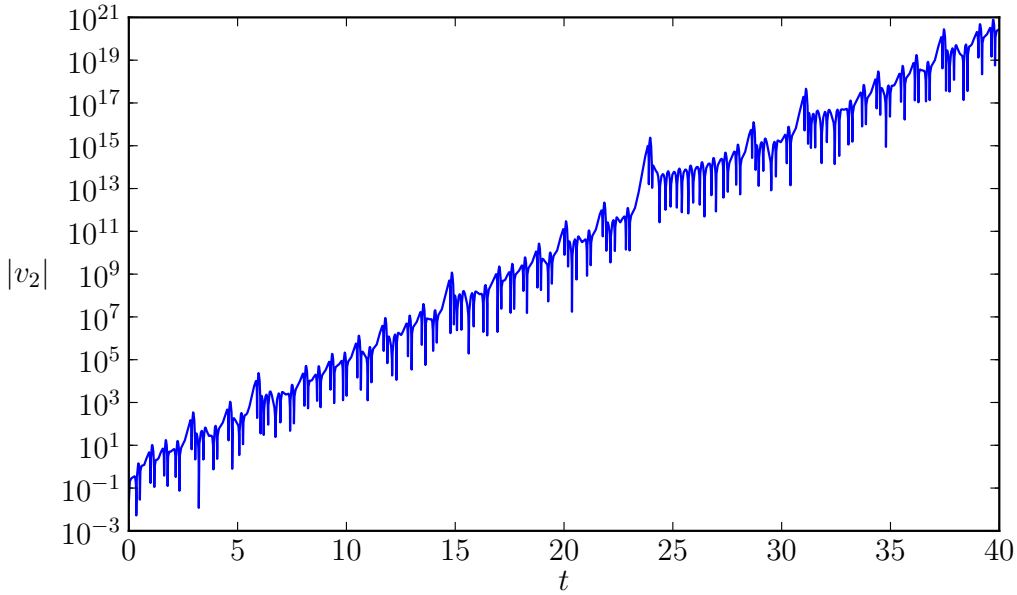

Figure 3 Absolute value of a component of the conventional tangent sensitivity for the Lorenz system and objective (7) **plotted against time. Note log scale on the y-axis.**

III. Proposed stabilization method

A. Method description and application to the Lorenz system

As Figure 3 demonstrates, the tangent sensitivity equation is linearly unstable for chaotic flows [20]. Therefore, our goal is to investigate how to modify the equation so that we can, hopefully, bound the "energy" in the tangent sensitivity $\mathbf{v}$; here, energy refers to the L^2 norm of the tangent sensitivity. Ideally, we seek modifications that stabilize the sensitivity without having a detrimental impact on gradient accuracy.

To discuss the modifications, we consider the generic initial value problem (2). To obtain an equation for the tangent sensitivity, we take the derivative of (2) with respect to the design variable s, which yields

$$\frac{d\mathbf{v}}{dt} - \left(\frac{\partial \mathbf{f}}{\partial \mathbf{u}}\right)\mathbf{v} - \frac{\partial \mathbf{f}}{\partial s} = 0, \qquad v(0) = 0, \tag{8}$$

where we have defined the tangent sensitivity as $\mathbf{v} = d\mathbf{u}/ds$.

Again, we are concerned with bounding the "energy" (the L^2 norm) of the tangent sensitivity. For the relevant energy analysis, it is sufficient to study the homogeneous form of (8), that is, where $\partial\mathbf{f}/\partial s$ is neglected. Left multiplying the homogeneous form of (8) by the tangent sensitivity transposed gives

$$\frac{d}{dt}\left(\frac{1}{2}\|\mathbf{v}\|^2\right) - \frac{1}{2}\mathbf{v}^T\left[\left(\frac{\partial \mathbf{f}}{\partial \mathbf{u}}\right) + \left(\frac{\partial \mathbf{f}}{\partial \mathbf{u}}\right)^T\right]\mathbf{v} - \frac{1}{2}\mathbf{v}^T\left[\left(\frac{\partial \mathbf{f}}{\partial \mathbf{u}}\right) - \left(\frac{\partial \mathbf{f}}{\partial \mathbf{u}}\right)^T\right]\mathbf{v} = 0, \tag{9}$$

where we have decomposed the Jacobian, $\partial\mathbf{f}/\partial\mathbf{u}$, into its symmetric and skew-symmetric parts. The skew-symmetric part does not contribute to the energy growth of $\mathbf{v}$, because $\mathbf{v}^T\mathsf{A}\mathbf{v} = -\mathbf{v}^T\mathsf{A}\mathbf{v} = 0$ for any skew-symmetric matrix A. We can therefore consider (9) without the skew-symmetric part of $\partial\mathbf{f}/\partial\mathbf{u}$:

$$\frac{d}{dt}\left(\frac{1}{2}\|\mathbf{v}\|^2\right) - \frac{1}{2}\mathbf{v}^T\left[\left(\frac{\partial \mathbf{f}}{\partial \mathbf{u}}\right) + \left(\frac{\partial \mathbf{f}}{\partial \mathbf{u}}\right)^T\right]\mathbf{v} = 0. \tag{10}$$

It follows from (10) that, in order to ensure energy stability, the following must be satisfied:

$$\mathbf{v}^T\left[\left(\frac{\partial \mathbf{f}}{\partial \mathbf{u}}\right) + \left(\frac{\partial \mathbf{f}}{\partial \mathbf{u}}\right)^T\right]\mathbf{v} \leq 0. \tag{11}$$

We seek to enforce this inequality by adding a symmetric matrix S to the Jacobian such that

$$\mathbf{v}^T\left(\frac{\partial \mathbf{f}}{\partial \mathbf{u}} + \mathsf{S}\right)\mathbf{v} \leq 0. \tag{12}$$

We will consider two different choices for S.

For the first choice, we seek the smallest S — in the sense defined below in (13) — that ensures the tangent sensitivity at a given time step satisfies (12). This S is given by the solution to the following quadratic optimization problem:

$$\begin{aligned} \min_{\mathsf{S}} \quad & \frac{1}{2}\sum_{i=1}^{n}\sum_{j=i}^{n}\mathsf{S}_{ij}^2 \\ \text{s.t.} \quad & \mathbf{v}^T\left(\frac{\partial \mathbf{f}}{\partial \mathbf{u}} + \mathsf{S}\right)\mathbf{v} \leq 0. \end{aligned} \tag{13}$$

Since (13) is a quadratic program with a convex objective, it has a closed-form solution. Additionally, we only solve (13) if the inequality is violated; otherwise, we set $\mathsf{S} = 0$. Note that, since (13) depends on the tangent sensitivity via the constraint, this stabilization approach is nonlinear.

The second, alternative, choice for S involves modifying the eigenvalues in the Jacobian. Positive eigenvalues in the Jacobian contribute to the unbounded growth of the tangent sensitivity. Therefore, our goal with the second stabilization method is to clip these positive eigenvalues. To this end, we perform the eigendecomposition

$$\left[\left(\frac{\partial \mathbf{f}}{\partial \mathbf{u}}\right) + \left(\frac{\partial \mathbf{f}}{\partial \mathbf{u}}\right)^T\right] = \mathsf{E}\lambda\mathsf{E}^\mathsf{T}, \tag{14}$$

where E is a matrix composed of the eigenvectors of the symmetric part of $\partial\mathbf{f}/\partial\mathbf{u}$, and λ is a diagonal matrix with the eigenvalues of the symmetric part of $\partial\mathbf{f}/\partial\mathbf{u}$ on the diagonal. Recall that we add S to the Jacobian, so we use S to eliminate positive eigenvalues; to do this, we set the negative eigenvalues in λ to zero, and we will refer to the modified diagonal matrix as λ^+. We then form the stabilization matrix $\mathsf{S}_{\mathsf{clip}}$ according to

$$\mathsf{S}_{\mathsf{clip}} = -\mathsf{E}\lambda^{+}\mathsf{E}^{\mathsf{T}}. \tag{15}$$

Although this eigenvalue-clipping stabilization modifies the tangent sensitivity equation more than the first approach, it is useful for comparison and shows promise on the model problem. It also maintains the linearity of the sensitivity equation.

B. Results on the model problem

To assess our methods' capacity for stabilization and subsequent impact on the total derivative, we apply them to the Lorenz system. The objective function remains the same as in Section II.B. We consider two time-stepping methods to more thoroughly investigate the stabilization methods for both implicit and explicit time-marching schemes; for the present study we have selected the implicit Crank-Nicolson scheme and the explicit 4th-order Runge-Kutta method. Our chosen range of interest for the design variable is $\rho = [30, 50]$, and we have calculated the objective function throughout this range at steps of $\Delta\rho = 0.01$. Stabilized gradients were evaluated at steps of $\Delta\rho = 2.0$. All solutions of the Lorenz system were obtained using a maximum time horizon of $T = 40$, and a time-step of $\Delta t = 0.004$. The objective function and stabilized gradients used the same time horizon. A spin-up period of 1000 time steps was used before beginning the statistics gathering period, in order to reduce the influence of the initial transients on the objective.

When applied to the Lorenz system with the Crank-Nicolson scheme, the two stabilization methods bound the tangent sensitivity; Figure 4 plots $|v_2|$ over time and demonstrates that the stabilized tangent sensitivity does not grow exponentially. In a similar fashion, our method bounds the tangent sensitivity when the Lorenz system is solved with the 4th-order Runge-Kutta method.

Gradients obtained from both stabilizations, based on the Crank-Nicolson scheme, are shown in Figures 5a and 5b. We see similar gradient information produced by the eigenvalue-clipping stabilization when the 4th-order Runge-Kutta method is used to solve the problem, shown in Figures 6a. Compared with the other results, larger errors are present in the gradients acquired through quadratic-program stabilization (Figure 6b) obtained using the 4th-order Runge-Kutta method. This is likely due to the aforementioned nonlinearity of this stabilization technique; nevertheless, the gradients remain bounded and approximate the general trend of the objective.

IV. Extension to computational fluid dynamics

The proposed method is promising, but it is not immediately clear that it will generalize to the Euler or Navier-Stokes equations. In particular, the perturbations to the Jacobian used in the Lorenz example relied on either a) solving a quadratic optimization with as many variables as the (symmetric part of the) Jacobian, or b) an eigen-decomposition of the Jacobian. In the case of an Euler or Navier–Stokes simulation, the Jacobian will have potentially billions (or more) of rows and columns, making such methods impractical.

In the following section, we explain why this issue is mitigated by the nature of the instability in fluid flows. Subsequently, we describe a practical implementation of the stabilization method in the case of the Euler equations.

A. A localized instability

As described in the introduction to this section, the proposed stabilization method appears to be impractical for the Euler or Navier-Stokes equations, because the size of the Jacobian matrix precludes the necessary optimization or eigen-decomposition. Fortunately, the terms responsible for destabilizing the Euler and Navier-Stokes sensitivities are spatially-local source terms. To see this, consider the (homogeneous) adjoint equation for the incompressible Navier–Stokes equations (with the summation-convention on repeated indices):

$$\rho\frac{\partial\psi_i}{\partial t} + \rho u_j\frac{\partial\psi_i}{\partial x_j} - \underbrace{\rho\frac{\partial u_j}{\partial x_i}\psi_j}_{\text{unstable}} + \frac{\partial\pi}{\partial x_i} = \nu\frac{\partial^2\psi_i}{\partial x_j\partial x_j}, \qquad \frac{\partial\psi_j}{\partial x_j} = 0, \tag{16}$$

where $\psi = [\psi_1, \psi_2, \psi_3]^T$ is the adjoint corresponding to velocity and π is the adjoint corresponding to pressure. Using an energy-stability analysis, Wang and Gao [20] showed that the third term in this equation is responsible for the adjoint's

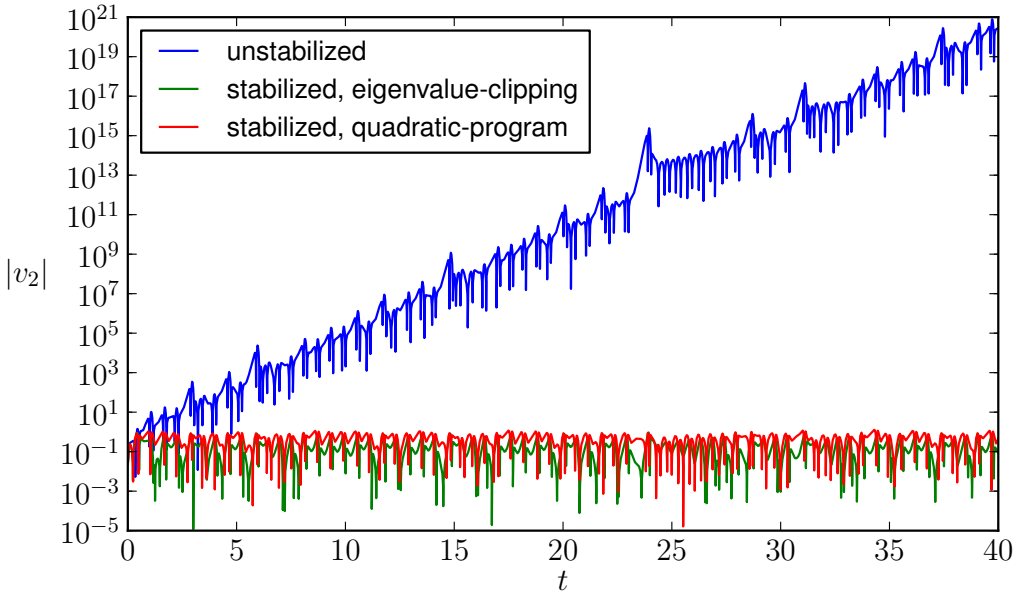

Figure 4 Comparison of a stabilized and unstabilized tangent sensitivity component for the Lorenz system and objective (7) plotted against time. Here, the Crank-Nicolson method was used to time march the solution, and both stabilizations are shown. Note log scale on the y-axis.

exponential growth. The symmetric part of the tensor multiplying ψ in the unstable term is

$$\frac{\rho}{2}\left(\frac{\partial u_i}{\partial x_j}+\frac{\partial u_j}{\partial x_i}\right),$$

which is the density times the strain-rate tensor. While this tensor depends on derivatives of the velocity field, it is entirely local from the perspective of the adjoint. Therefore, we can perturb this small, 3×3 tensor at each node in exactly the same way that we did to stabilize the tangent sensitivity of the Lorenz system.

Talnikar *et al.* [19] performed an energy-stability analysis of the compressible Navier–Stokes adjoint and showed that its destabilizing term is also a spatially localized source term. Consequently, the proposed approach is equally valid for stabilizing the types of flow problems of interest to the aerospace industry.

At this point, it is worth highlighting the differences between the proposed stabilization and the dissipation-based stabilization used in [19]. Introducing dissipation into the adjoint requires a subtle balance between stabilizing the equation and obtaining accurate sensitivities: too little dissipation and the tangent or adjoint will grow exponentially, too much dissipation and the sensitivities will be inaccurate. The difficulty in achieving this balance was documented in [19].

In contrast, the proposed stabilizations are, in some sense, the minimum perturbations necessary to avoid exponential growth in the tangent or adjoint. Our hypothesis is that such perturbations will lead to sufficiently accurate sensitivities, as they did for the Lorenz problem. Furthermore, the proposed methods are parameter-free, which is a significant advantage in practice.

B. Implementation case-study: SBP discretization of the Euler equations

The proposed stabilization(s) can be applied to a wide range of discretizations, but the details will vary depending on the choice of discretization. For concreteness, we will focus on an entropy-stable summation-by-parts (SBP) discretization. Furthermore, the destabilizing term in the sensitivity equations, for both incompressible and compressible flows, is due to the inviscid terms. Therefore, to describe our implementation it is sufficient to consider the Euler equations. Finally, since the destabilization mechanism is the same for both the tangent and adjoint sensitivity, we will consider the tangent sensitivity for simplicity.

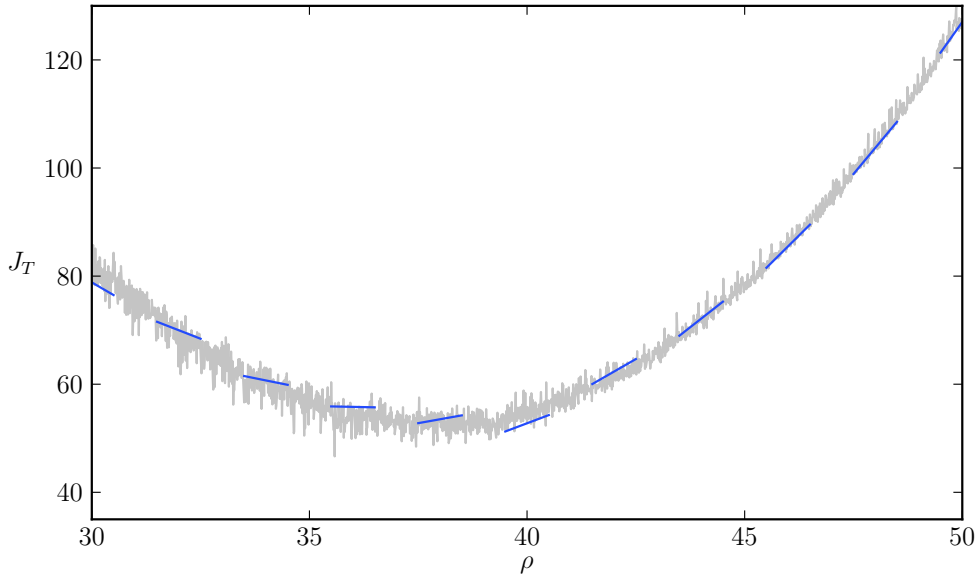

(a) CN, eigenvalue-clipping stabilization

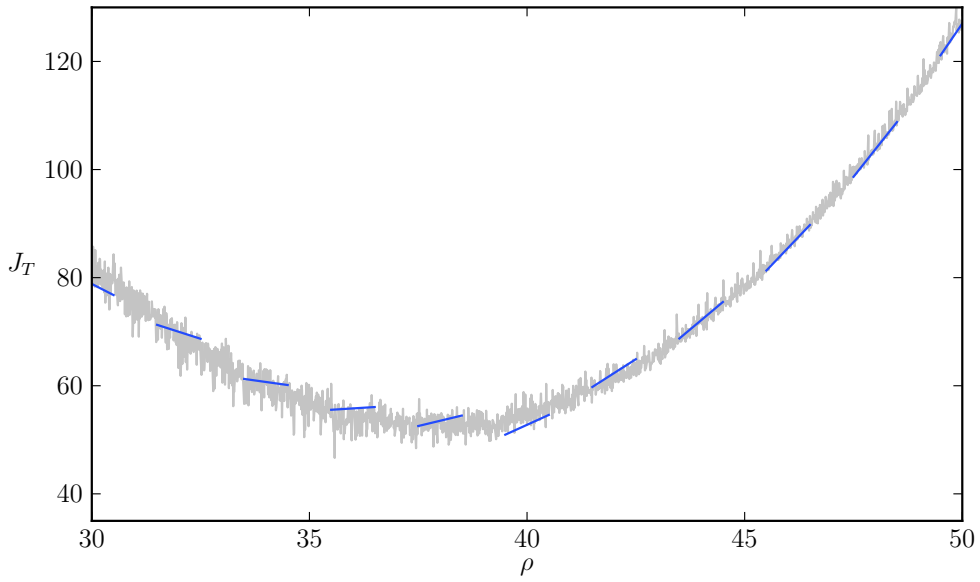

(b) CN, quadratic-program stabilization

Figure 5 The stabilizations applied to the Lorenz system, solved with the Crank-Nicolson (CN) time-stepping method. Both stabilization methods are shown. The objective function is plotted against ρ in grey, and plotted in blue are linearizations of the gradients obtained through our stabilization methods applied to the tangent sensitivity method.

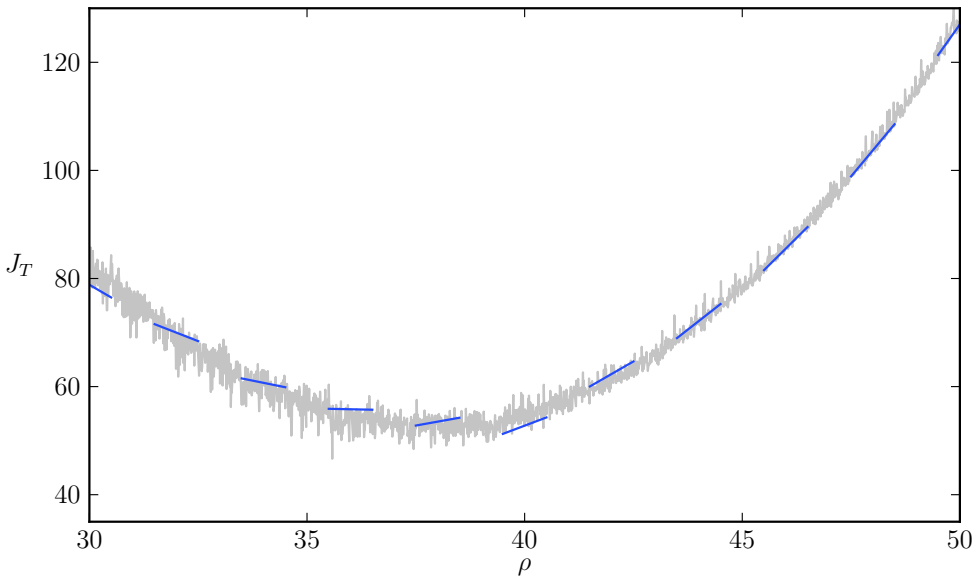

(a) RK4, eigenvalue-clipping stabilization

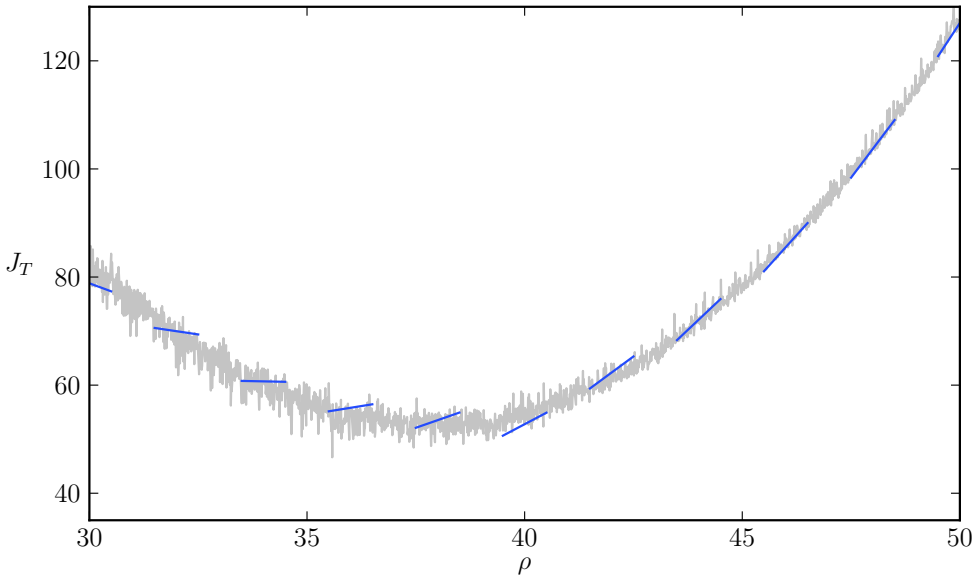

(b) RK4, quadratic-program stabilization

Figure 6 **The stabilizations applied to the Lorenz system, solved with the 4th-order Runge-Kutta (RK4) time-stepping method. Both stabilization methods are shown. As in Figure 5, the objective function is plotted against ρ in grey, and plotted in blue are linearizations of the gradients obtained through our stabilization methods applied to the tangent sensitivity method.**

The entropy-stable SBP discretization of the Euler equations [21] produces a semi-discretization of the form

$$\mathsf{H}\frac{d\mathbf{u}_h}{dt} - \sum_{\kappa\in\mathcal{T}} \mathsf{P}_\kappa^T \mathbf{F}_\kappa(\mathsf{P}_\kappa \mathbf{u}_h) - \mathbf{b}(\mathbf{u}_h, s) = 0, \tag{17}$$

where $\mathbf{u}_h(t) \in \mathbb{R}^n$ is the discrete solution evaluated at the collocation points, and $s \in \mathbb{R}$ is a parameter, as before. Here we consider a continuous SBP solution space over the tesselation of the domain $\mathcal{T}$, which is analogous to a continuous Galerkin finite-element method (in contrast with the discontinuous SBP space considered in [21]). The matrix $\mathsf{H} \in \mathbb{R}^{n\times n}$ is the diagonal mass matrix, the matrix $\mathsf{P}_\kappa \in \mathbb{R}^{n_\kappa \times n}$ restricts the global solution to the n_κ degrees of freedom on element κ, and $\mathbf{F}_\kappa : \mathbb{R}^{n_\kappa} \to \mathbb{R}^{n_\kappa}$ denotes the element-local residual vector that discretizes the spatial derivatives. Finally, $\mathbf{b} : \mathbb{R}^n \times \mathbb{R} \to \mathbb{R}^n$ denotes the boundary terms; the boundary conditions are imposed weakly using penalty terms and we assume they depend on the parameter s.

As usual, the tangent-sensitivity equation is obtained by (total) differentiation of the discretization (17) with respect to s. Thus, if $\mathbf{v}_h(t) \in \mathbb{R}^n$ denotes the sensitivity, the tangent-sensitivity equation is given by

$$\mathsf{H}\frac{d\mathbf{v}_h}{dt} - \sum_{\kappa\in\mathcal{T}} \mathsf{P}_\kappa^T \mathsf{J}_\kappa \mathsf{P}_\kappa \mathbf{v}_h - \frac{\partial \mathbf{b}}{\partial \mathbf{u}_h}\mathbf{v}_h - \frac{\partial \mathbf{b}}{\partial s} = 0, \tag{18}$$

where $\mathsf{J}_\kappa \equiv \partial \mathbf{F}_\kappa / \partial \mathbf{u}_\kappa$ is the element-local Jacobian, with $\mathbf{u}_\kappa = \mathsf{P}_\kappa \mathbf{u}_h$. In the following analysis, we will focus on stabilizing the terms involving J_κ, since they contain the localized instability described earlier. We will not stabilize the derivatives of the boundary terms, which are responsible for driving the tangent (and adjoint) sensitivities.

Next, we perform an energy-stability analysis of (18). Ignoring the boundary-term derivatives and left-multiplying by $\mathbf{v}_h^T$, we find

$$\begin{aligned} & \mathbf{v}_h^T \mathsf{H}\frac{d\mathbf{v}_h}{dt} - \sum_{\kappa\in\mathcal{T}} \mathbf{v}_h^T \mathsf{P}_\kappa^T \mathsf{J}_\kappa \mathsf{P}_\kappa \mathbf{v}_h = 0 \\ \Rightarrow \qquad & \frac{d}{dt}\left(\frac{1}{2}\|\mathbf{v}_h\|_{\mathsf{H}}^2\right) = \sum_{\kappa\in\mathcal{T}} \mathbf{v}_\kappa^T \mathsf{J}_\kappa \mathbf{v}_\kappa, \end{aligned}$$

where $\|\mathbf{v}_h\|_{\mathsf{H}}$ is the SBP approximation of the L^2 norm of $\mathbf{v}_h$, and $\mathbf{v}_\kappa \equiv \mathsf{P}_\kappa \mathbf{v}_h$ is the tangent sensitivity projected onto the degrees of freedom of element κ. In general, $\mathbf{v}_\kappa^T \mathsf{J}_\kappa \mathbf{v}_\kappa$ may be positive, leading to growth in the sensitivity. To combat this, following the Lorenz-problem example, we add a symmetric matrix $\mathsf{S}_\kappa \in \mathbb{R}^{n_\kappa \times n_\kappa}$ to each J_κ such that $\mathbf{v}_\kappa^T(\mathsf{J}_\kappa + \mathsf{S}_\kappa)\mathbf{v}_\kappa \le 0$. It then follows that

$$\frac{d}{dt}\left(\frac{1}{2}\|v_h\|_{\mathsf{H}}^2\right) = \sum_{\kappa\in\mathcal{T}} \mathbf{v}_\kappa^T(\mathsf{J}_\kappa + \mathsf{S}_\kappa)\mathbf{v}_\kappa \le 0,$$

which implies the tangent sensitivity remains bounded. The element-level matrices S_κ are found using one of the two stabilization methods described earlier: solving a quadratic optimization analogous to (13), or; using S_κ to remove the positive eigenvalues from the symmetric part of J_κ.

Notice that, rather than stabilizing the global Jacobian, $\sum_{\kappa\in\mathcal{T}} \mathsf{P}_\kappa^T \mathsf{J}_\kappa \mathsf{P}_\kappa$, we instead stabilize $|\mathcal{T}|$ element Jacobians, J_κ. This represents a significant reduction in cost, since the former requires perturbations to a Jacobian with $\mathrm{O}(n^2)$ entries, while the latter requires perturbations to an element Jacobian with only $\mathrm{O}(n_\kappa^2)$ entries. Furthermore, the element stabilization is easily parallelized.

V. Summary & Future work

Gradient-based optimization algorithms breakdown in the presence of chaos, because conventional sensitivity analysis methods cannot provide useful gradients due to exponential growth of the tangent and adjoint sensitivities. To address this problem, we have developed two methods of stabilizing the tangent (or adjoint) sensitivity equations. One method calculates the minimum possible perturbation to the symmetric part of the Jacobian to ensure energy stability, while the other method clips the positive eigenvalues of the symmetric part of the Jacobian. The methods were successfully applied to stabilize the tangent-sensitivity equation for the Lorenz ordinary differential equation.

The ultimate goal of this work is gradient-based aerodynamic shape optimization of turbulent, and therefore chaotic, flows. Keeping this goal in mind, we have described how the stabilization methods can be extended to CFD problems. In

particular, we have described how the methods remain computationally tractable in the context of an summation-by-parts discretization of the Euler equations. Future investigations of this stabilization will involve its application to CFD problems, such as the airfoil case presented by Blonigan *et al.* [23].

VI. Acknowledgements

A. Ashley and J. Hicken gratefully acknowledge the support of the Air Force Office of Scientific Research Award FA9550-15-1-0242 under Dr. Jean-Luc Cambier and Dr. Fariba Fahroo. We also thank RPI's Scientific Computation Research Center and Center for Computational Innovation for the use of computer facilities.

References

[1] Lyness, J. N., and Moler, C. B., "Numerical Differentiation of Analytic Functions," *SIAM Journal of Numerical Analysis*, 1967, pp. 202-210.

[2] Lions, J-L., "Contrôle optimal de systèmes gouvernés par des équations aux dérivées partielles," *Etudes Mathématiques*, Dunod; Gauthier-Villars, Collier-Macmillan Ltd.

[3] Jameson, A., "Aerodynamic design via control theory," *Journal of Scientific Computing*, Sep. 1988, Vol. 3, Iss. 3, pp. 233-260.

[4] Nadarajah, S. K., and Jameson, A. "Optimum Shape Design for Unsteady Flows with Time-Accurate Continuous and Discrete Adjoint Method," *AIAA Journal*, Vol. 45, No. 7 (2007), pp. 1478-1491.

[5] Duta, M. C., Giles, M. B., and Campobasso, M. S., "The harmonic adjoint approach to unsteady turbomachinery design," *Intermational Journal for Numerical Methods in Fluids*, Sep. 2002, Vol. 40, No. 3-4, pp. 323-332.

[6] Rumpfkeil, M. P., and Zingg, D. W., "The optimal control of unsteady flows with a discrete adjoint method," *Optimization and Engineering*, Feb. 2010, Vol. 11, Iss. 1, pp 5–22.

[7] Wang, L., Mavriplis, D. J., and Anderson, W. K., "Adjoint Sensitivity Formulation for Discontinuous Galerkin Discretizations in Unsteady Inviscid Flow Problems," *AIAA Journal*, Dec. 2010, Vol. 48, No. 12.

[8] Lorenz, E. N., "Deterministic Nonperiodic Flow," *Journal of The Atmospheric Sciences*, Mar. 1963, pp. 130-141.

[9] Lea, D. J., Allen, M. R., and Haine, T. W. N., "Sensitivity analysis of the climate of a chaotic system," *Tellus: Series A, Dynamic Meteorology and Oceanography*, Oct. 2000, Vol. 52, No. 5, pp. 523-532.

[10] Ashley, A., and Hicken, J. E., "Optimization Algorithm for Systems Governed by Chaotic Dynamics," *AIAA Aviation Conference*, 2014, AIAA 2014-2434.

[11] Eyink, G. L., Haine, T. W. N, and Lea, D. J., "Ruelle's linear response formula, ensemble adjoint schemes and Lévy flights," *Nonlinearity*, Sep. 2004, Vol. 17, No. 5., pp. 1867+.

[12] Chandramoorthy, N., Fernandez, P., Talnikar, C., and Wang, Q., "The Ensemble Adjoint Method for Chaotic CFD: A Feasibility Study," *23rd AIAA Computational Fluid Dynamics Conference*, AIAA Aviation Forum, Jun. 5-9 2017.

[13] Blonigan, P., Gomez, S., and Wang, Q., "Least Squares Shadowing for Sensitivity Analysis of Turbulent Fluid Flows," *AIAA Scitech Conference*, 2014, `https://arxiv.org/abs/1401.4163`.

[14] Liao, H. "Efficient sensitivity analysis method for chaotic dynamical systems," *Journal of Computational Physics*, 2016, Vol. 313, pp. 57-75.

[15] Ashley, A., and Hicken, J. E., "Sensitivity Analysis of Chaotic Problems using a Fourier Approximation of the Least-Squares Adjoint," *AIAA Aviation Conference*, 2016, 17th AIAA/ISSMO Multidisciplinary Analysis and Optimization Conference.

[16] Ni, A., Blonigan, P. J., Chater, M., and Wang, Q., "Sensitivity analysis on chaotic dynamical system by Non-Intrusive Least Square Shadowing (NI-LSS)," *AIAA Aviation Conference*, 2016, 46th AIAA Fluid Dynamics Conference, AIAA 2016-4399.

[17] Blonigan, P. J., Wang, Q., Nielsen, E. J., and Diskin, B., "A non-intrusive algorithm for sensitivity analysis of chaotic flow simulations," *AIAA SciTech Conference*, 2017, 55th AIAA Aerospace Sciences Meeting, AIAA 2017-0532.

[18] Ni, A., and Wang, Q., "Sensitivity analysis on chaotic dynamical systems by Non-Intrusive Least Squares Shadowing (NILSS)", *Journal of Computational Physics*, Vol. 347, pp. 56-77, 2017.

[19] Talnikar, C., Wang. Q., and Laskowski, G. M., “Unsteady Adjoint of Pressure Loss for a Fundamental Transonic Turbine Vane," *Journal of Turbomachinery*, Mar. 2017, Vol. 139.

[20] Wang, Q., and Gao, J-H., “The drag-adjoint field of a circular cylinder wake at Reynolds numbers 20, 100 and 500," *Journal of Fluid Mechanics*, Sep. 2013, Vol. 730, pp. 145-161.

[21] Crean, J., Hicken, J. E., Del Rey Fernández, D. C., Zingg, D. W., and Carpenter, M. H., “Entropy-stable summation-by-parts discretization of the Euler equations on general curved elements", *Journal of Computational Physics*, Mar. 2018, Vol. 356, pp. 410-438.

[22] Hicken, J. E., Fernández, D. D. R., and Zingg, D. W., “Multidimensional Summation-by-Parts Operators: General Theory and Application to Simplex Elements", *Methods and Algorithms for Scientific Computing*, SIAM J. Sci. Comput., 38(4), A1935–A1958.

[23] Blonigan, P. J, Wang, Q., Nielsen, E. J., and Diskin, B., “Least-Squares Shadowing Sensitivity Analysis of Chaotic Flow Around a Two-Dimensional Airfoil", *AIAA Journal*, Vol. 56, No. 2 (2018), pp. 658-672.